BIOCHEMISTRY
including biophysical chemistry & molecular biology

Article

pubs.acs.org/biochemistry

The Catalytic Mechanism of Carboxylesterases: A Computational Study

J. Aranda,[‡,§] N. M. F. S. A. Cerqueira,[†,§] P. A. Fernandes,[†] M. Roca,[‡] I. Tuñon,*[,‡] and M. J. Ramos*[,†]

[†]REQUIMTE, Departamento de Química e Bioquímica, Faculdade de Ciências, Universidade do Porto, Rua do Campo Alegre s/n, 4169-007 Porto, Portugal

[‡]Departament de Química Física, Universitat de València, 46100 Burjassot, Spain

Supporting Information

ABSTRACT: The catalytic mechanism of carboxylesterases (CEs, EC 3.1.1.1) is explored by computational means. CEs hydrolyze ester, amide, and carbamate bonds found in xenobiotics and endobiotics. They can also perform transesterification, a reaction important, for instance, in cholesterol homeostasis. The catalytic mechanisms with three different substrates (ester, thioester, and amide) have been established at the M06-2X/6-311++G**//B3LYP/6-31G* level of theory. It was found that the reactions proceed through a mechanism involving four steps instead of two as is generally proposed: (i) nucleophilic attack of serine to the substrate, forming the first tetrahedral intermediate, (ii) formation of the acyl−enzyme complex concomitant with the release of the alcohol product, (iii) nucleophilic attack of a water or alcohol molecule forming the second tetrahedral intermediate, and (iv) the release of the second product of the reaction. The results agree very well with the available experimental data and show that the hydrolytic and the transesterification reactions are competitive processes when the substrate is an ester. In all the other studied substrates (thioester or amide), the hydrolytic and transesterification process are less favorable and some of them might not even take place under *in vivo* conditions.

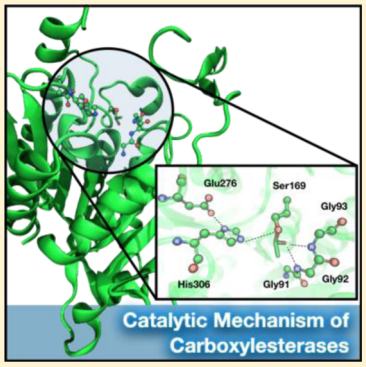

Carboxylesterases are members of the esterase class of proteins (EC 3.1.1.1 for CEs) that cleave carboxyesters (RCOOR′) into the corresponding carboxylic acid (RCOOH) and alcohol (R′OH) via a proton transfer hydrolysis mechanism using a catalytic serine present within a Ser-His-Glu triad. These enzymes are widely distributed in nature and especially common in mammalian liver (Scheme 1) displaying different roles.[1−16] Mammalian CEs are promiscuous enzymes that hydrolyze esters, thioesters, and amide-ester linkages of a broad spectrum of structurally diverse compounds.[1,2] This includes clinical drugs such as the cholesterol-lowering drug lovastatin[3] and the local anesthetic and antiarrhythmic lidocaine,[4] anticancer drugs such as CPT-11 and capecitabine,[5] the antibiotics Ceftin and Vantin, and the angiotensin-converting enzyme inhibitors delapril, imidapril, and temocapril.[6] The dangerous narcotics heroin and cocaine, as well as the potent chemical weapon agents sarin, soman, and tabun, can be metabolized and detoxified by CEs too.[1,7,8] This family of enzymes has been associated also with cholesterol and fatty acid metabolism where they play crucial roles. Some examples are the fatty acyl CoA hydrolase,[9] acyl CoA cholesterol acyl transferase,[10] cholesterol ester hydrolase,[11] acyl carnitine hydrolase,[12] fatty acyl ethyl ester synthase,[13] and triacylglycerol hydrolase.[14] Furthermore, it has been proposed that CEs might play specific roles in lung surfactant[15] and pheromone metabolism.[16]

The ability to bind different substrates exhibited by CEs allows the cell to metabolize a wide variety of compounds. However, the lack of specificity generally results in relatively high K_M values and low catalytic efficiencies (k_{cat}/K_M) for hydrolysis of drugs or environmental esters. The low catalytic efficiency is usually compensated by the presence of relatively large amounts of these enzymes in tissues, especially in the liver.[17]

The mechanism by which carboxylesterases hydrolyze their substrates has been examined by many researchers using both biochemical and structural means. The currently accepted mechanism is based on the proposals made by Satoh, Hosokawa, Sogorb, Vilanova, and Redinbo[1,7,18−20] (Scheme 1). According to these authors, the cleavage of the ester group is base-mediated, requiring water as a coreactant. The reaction is achieved via a triad of catalytic amino acids (Ser169, Glu276, and His306) that are highly conserved among carboxylesterases and are essential for the enzymatic activity.[8] At neutral pH, the side chain carboxylic group of the active site glutamic residue is negatively charged, a condition that facilitates the accommodation of a positive charge in the histidine accepting the proton belonging to the serine residue. This proton transfer from Ser169 to the opposing nitrogen of His306 generates an oxygen nucleophile that can attack the carbonyl carbon of the substrate. When the tetrahedral intermediate of an acyl group is formed, the alcohol product is released from the enzyme. The acyl−

Received: July 29, 2014
Revised: August 6, 2014
Published: August 7, 2014

   dx.doi.org/10.1021/bi500934j | *Biochemistry* 2014, 53, 5820−5829

Scheme 1. Schematic Representation of the Catalytic Mechanism of Mammalian Carboxylesterases[a]

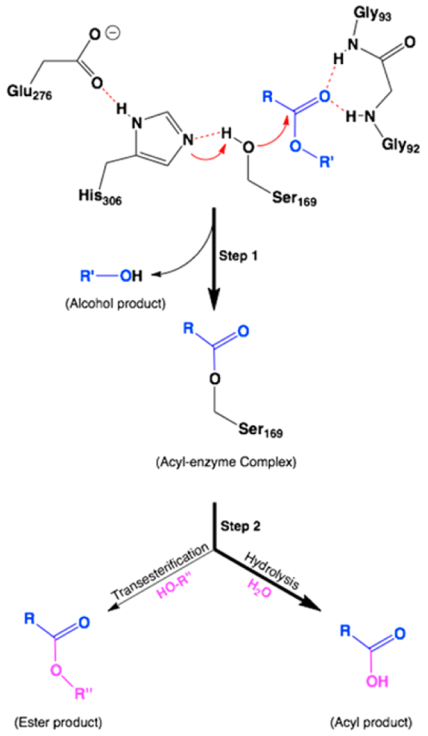

[a]The bold arrows represent the typical route of hydrolysis that is catalyzed by these enzymes.

enzyme intermediate is then attacked by a water molecule that acts as the nucleophile, leading to the release of the carboxylic acid and to enzymatic turnover. Several authors have reported that CEs also have the capability to perform transesterification reactions. This happens when alcohol molecules are abundant in the active site and compete with the water molecules during the attack to the acyl−enzyme intermediate. In these cases, at the end of the reaction, an ester group is obtained instead of a carboxylic acid (acyl product).

Although quite appealing, the proposed catalytic mechanism of CEs shown in Scheme 1 leaves a number of interesting questions unanswered. For instance, many authors suggest that the cleavage of the ester group occurs in two distinct steps, while others propose a concerted type of mechanism.[1,21,22] There is also much debate around the interaction between the glutamic acid and the histidine of the catalytic triad during the catalysis.[22,23] In addition it is suggested that nitrogen atoms of Gly92 and Gly93 may be part of an oxyanion hole that is essential for the formation of the tetrahedral intermediate.[1] Additionally, the transesterification mechanism is still poorly understood and requires further investigation.

In the present work, we have examined the catalytic mechanism of carboxylesterases using the density functional theory (DFT) functional B3LYP trying to unravel all these unanswered questions. These methods have been shown in the past to be quite successful to study enzymatic mechanisms and to retrieve many clues for further advances in the field.[24−28] In particular these methods allow one to unravel the energies involved in each step of the reaction and to acquire an atomic portrait of the full reaction, which is necessary to fully understand the catalytic power and substrate promiscuity of carboxylesterases with additional future research work.

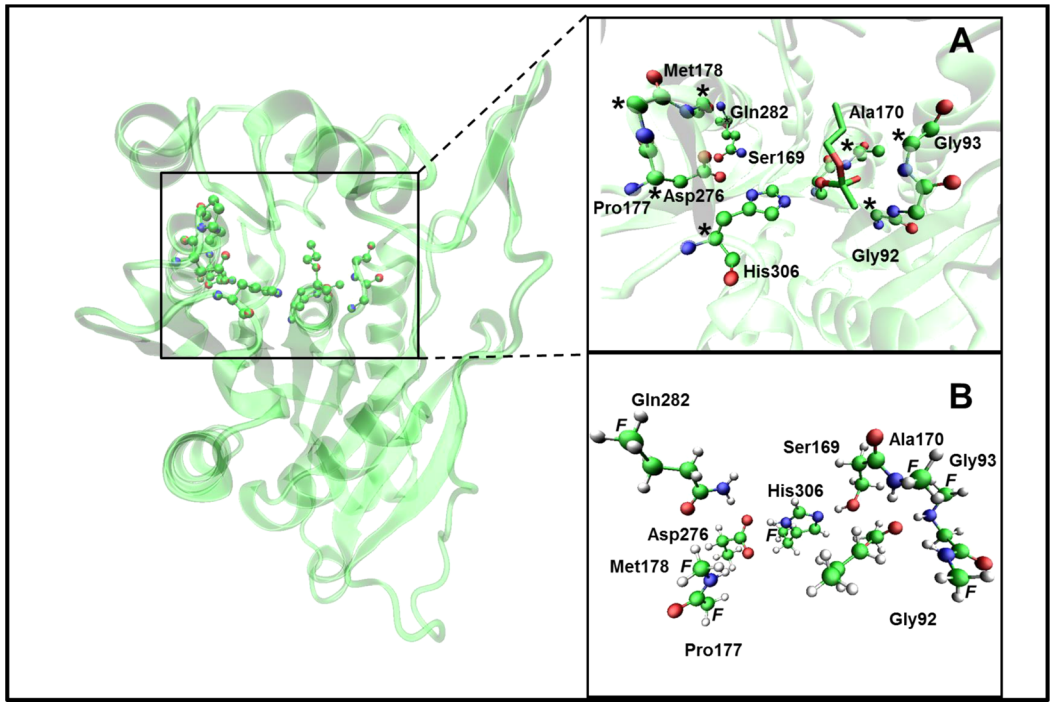

Figure 1. X-ray structure of carboxylesterase AeCXE1 from plant *Actinidia eriantha*. (A) The most important residues that take part in the reaction mechanism are represented in ball and sticks (the atoms that were truncated and replaced by methyl groups in the cluster model are marked with an asterisk). The covalent intermediate (propyl acetate) is represented in sticks. (B) Cluster model used in the computational studies (the atoms that were frozen during the geometry optimizations are highlighted with the letter *F*).

dx.doi.org/10.1021/bi500934j | *Biochemistry* 2014, 53, 5820−5829

METHODOLOGY

The initial coordinates were taken for the X-ray structure of plant carboxylesterase AeCXE1 (pdb code 2O7R), which is crystallized with a tetrahedral intermediate for the reaction with the propyl acetate substrate.[29] We then built what is known as an active site model, selecting the main residues involved in the reaction.[30−32] This model consisted of the propyl acetate, the side chain of the Ser169 residue, part of the backbone of Ala170, the side chain of Asp276, the side chain of His306, the backbone of Gly92, part of the backbone of Gly93, the side chain of Gln282, and part of the backbone of both Pro177 and Met178. The total number of atoms in the model varies between 103 and 93 atoms in total, according to the type of substrate that was studied, for example, propyl acetate, *S*-propyl ethanethioate, and *N*-propylacetamide. The coordinates of the starting models were deposited as Supporting Information.

The model (see Figure 1) was then subjected to geometry optimizations. In this process, some atoms (marked in the figure) were constrained to keep the geometry of the cluster model close to what is observed in the X-ray structure.

All geometry optimizations were performed with Gaussian 09,[33] applying density functional theory.[34] Becke's three-parameter exchange functional was used together with the functional of Lee et al. (B3LYP)[35−37] as implemented in Gaussian and the 6-31G(d) basis set.[38] In all geometry optimizations, we first searched for the transition state starting from a structure similar to the reactant model. This was generally obtained with unidimensional scans along the particular reaction coordinate in which we were interested. Once a putative transition structure was located, and thus was fully optimized (except for the frozen atoms), the reactants and the products associated with it were determined after intrinsic reaction coordinate (IRC) calculations. In all cases, the geometry optimizations and the stationary points were obtained with standard Gaussian convergence criteria. The transition state structures were all verified by vibrational frequency calculations, having exactly one imaginary frequency with the correct transition vector, even using frozen atoms, which shows that the frozen atoms were almost free from steric strain. The ZPE and thermal and entropic energy corrections were calculated using the same method and basis set (T = 310.15 K, P = 1 bar).

The final electronic energies were calculated using the all-electron 6-311++G(3df,2pd) basis set and the functional M06-2X.[39,40] To estimate the interaction of the remaining enzyme in the reactions, single point energy calculations on the optimized geometries were performed with the conductor-like polarizable continuum model using the integral equation formalism variant (IEF-PCM),[41] as implemented in Gaussian 09, at the M06-2X/6-311++G(3df,2pd) level. This feature is of particular importance for the study of enzymatic catalysis because the use of a continuum model is normally taken as an approximation to the effect of the global enzyme environment in a reaction. A dielectric constant of ε = 4 was chosen to describe the protein environment of the active site according to previous suggestions.[28,42,43] A dielectric continuum can be a reasonable approximation to the effect of the enzyme environment if the most important specific (anisotropic) interactions are represented atomistically and only the longer-range, more isotropic interactions are modeled by the continuum.

All the activation and reaction energies provided in the text and figures refer to free energy differences calculated at the M06-2X/B3LYP/6-311++G(3df,2pd) level detailed above, while the atomic charge distributions were calculated at the B3LYP level by employing a Mulliken population analysis, using the basis set 6-31G(d).

RESULTS AND DISCUSSION

In this work, we unravel the catalytic mechanism of the mammalian CEs using quantum mechanical electronic structure calculations. Since there is no X-ray structure of this enzyme with good resolution for mammalian species, we based this study on the X-ray structure from plant carboxylesterase AeCXE1 from *Actinidia eriantha* (PDB code 2O7R).[29] We chose this structure because it has a better resolution (1.40 Å) and has a high sequence identity with the mammalian CEs (95%). Additionally, this structure was cocrystallized with a covalent intermediate (propyl acetate substrate), providing us a good starting point to study the catalytic mechanism.

We also superimposed the active sites corresponding to the plant and the mammalian X-ray structures and concluded that there were almost no differences between these structures and they can be almost completely overlapped.

The active site of this enzyme is located at the bottom of a hydrophobic and narrow tunnel, which is 11 Å away from the surface of the enzyme. In this region, we find the conserved catalytic triad of residues, constituted by Ser169, Asp 276, and His 306, and the oxyanion hole formed by Gly92, Gly93, and the backbone nitrogen atom of Ala170. The substrate binds in the active site with the ester group pointing toward the bottom region of the active site, nearby the region where the catalytic triad and the oxyanion hole region are located. The position of the substrate is stabilized by three hydrogen bonds provided by the NH groups of the two glycine residues and Ala170 that form the oxyanion hole. These interactions are very important because they align carbon C5 of the substrate with Ser169, a condition that is required to initiate the catalytic process (see Figure 1). Ser169 is located in a characteristic "nucleophilic elbow" position, providing enough mobility for this residue to interact with the substrate. We also included in our model the side chain of Gln282 residue and part of the backbone atoms of Pro177 and Met178. While oxygen atom Oδ2 of Asp276 forms a hydrogen bond with the Gln282 Nε2 atom, the Oδ1 atom of this residue is hydrogen bonded to the backbone nitrogen atom of Met178. This led to a conformational restraint of Asp276 and to the stabilization of its negative charge.

As mentioned above, apart from their hydrolytic capability, CEs can also catalyze transesterification reactions. In this work, we study both mechanisms. Since the first part of the mechanisms is common to both reactions, we present the results in three sections: (a) formation of the acyl−enzyme complex, (b) hydrolytic reaction, and (c) transesterification reaction. The first stage of the mechanism involves the formation of an acyl−enzyme complex in which an active site serine becomes covalently bound to the substrate. The second and third stages of the mechanism are dependent on the availability of water or alcohol in the active site. If water is available, then the hydrolytic reaction (normal pathway) will take place, and by the end of the reaction the substrate will be converted into an acyl product. If alcohol is available instead, then the transesterification process will take place, and by the end of the reaction an ester product is obtained.

dx.doi.org/10.1021/bi500934j | *Biochemistry* 2014, 53, 5820−5829

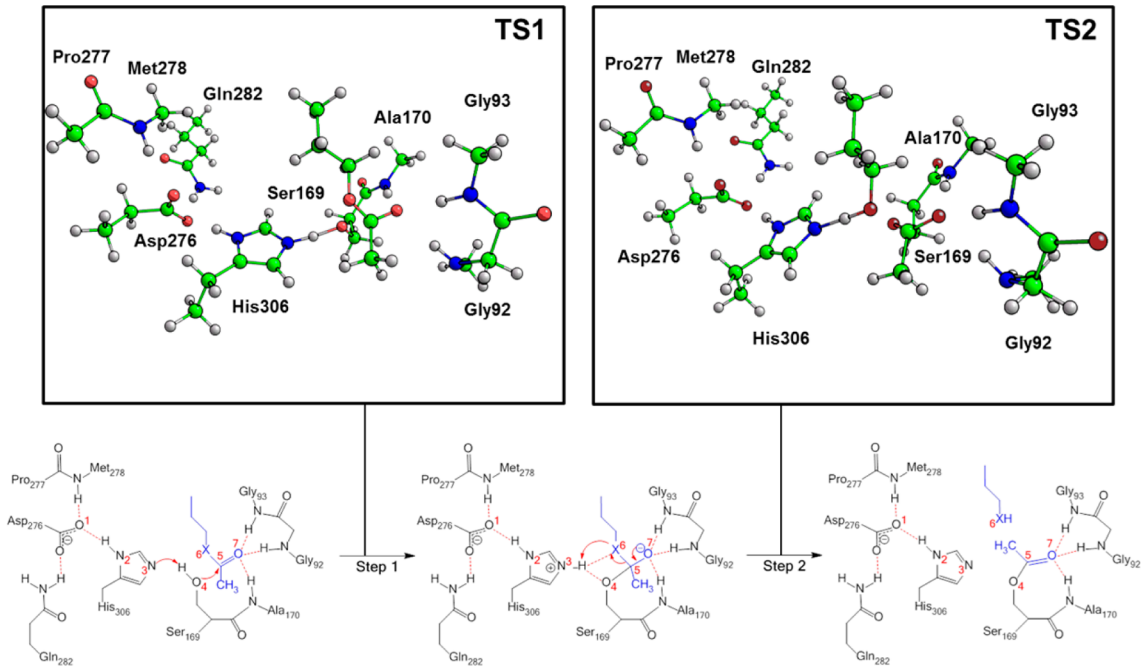

Figure 2. Formation of the acyl−enzyme complex and the release of the first product of the reaction catalyzed by CEs. (The TS images have the ester as substrate.)

Formation of the Acyl−Enzyme Complex. The formation of the acyl−enzyme complex requires the nucleophilic attack of Ser169 to the substrate and the concomitant formation of the first product of the reaction, an alcohol molecule. The computational results obtained in this study have shown that this process requires two sequential steps. In the optimized geometry of the reactant, the position of the substrate is similar to what is observed in the X-ray structure 2O7R. The carbonyl group establishes three hydrogen bond interactions: two of them with the backbone nitrogen atoms of Gly92 and Gly93 of the oxyanion hole region (1.79 and 2.11 Å respectively) and one with the backbone nitrogen atom of Ala170 (1.98 Å) (see Figure 2). Ser169 is very close to carbon C5 of the substrate (O4−C5 bond length of 2.33 Å, atom numbering given in Figure 2) and establishes a hydrogen bond with His306 (H4−N3 bond length of 1.59 Å). His306 and Asp276 interact very closely with each other through a short hydrogen bond (O1−H2 bond length 1.59 Å) with the charge mainly located at the Asp276 oxygen atom (the partial charge for this atom is −0.872 au). Also, Asp276 is hydrogen bonded through its Oδ1 atom with Gln282 nitrogen atom Nε with a distance of 1.60 Å and with nitrogen atom of the backbone of Met177 (1.95 Å). In the optimized structure of the transition state of the first step (frequency: 331i cm^{-1}), the proton that was firmly bonded to Ser169 is now shared with His306 (O4−H3 bond length of 1.36 versus 1.02 Å in the reactants). This increases the nucleophilic character of Ser169 that is now closer and ready to attack the substrate at carbon C5 (O4−C5 bond length of 1.88 versus 2.32 Å in the reactants). The hydrogen bond formed between Asp276 and His306 shortens its distance to 1.53 Å to accommodate the upcoming positive charge formed in the His306 residue. In the product of this step, this distance is more decreased to 1.49 Å (the total charge of Asp276 is −0.946 au). The proton that was previously bonded to Ser169 is now attached to His306, and Ser169 becomes covalently attached to the substrate at carbon C5 (O4−C5 bond length of 1.56 Å).

At this point, a separation of charges takes place, where the His306 becomes double protonated with a total charge of 0.793 au (versus 0.052 au in reactants structure), and the Ser169−substrate tetrahedral complex is negatively charged. This negatively charged adduct is stabilized in the active site by the net of hydrogen bonds that are provided by the Gly92, Gly93, and Ala170 backbone to the oxyanion pocket. This step requires an activation energy of 8.7 kcal/mol and a change in the overall energy of reaction of 2.5 kcal/mol.

The formation of the acyl−enzyme complex is not accomplished yet and requires a second step compromising the collapse of the tetrahedral intermediate and the release of the first product of the reaction, the alcohol product. In the reactants of this step, Ser169 remains firmly bonded to the substrate (O4−C5 bond length of 1.48 Å). Carbon C5 of the tetrahedral adduct complex remains bonded to three oxygen atoms (average bond length of 1.43 Å), and the new complex is negatively charged (total charge of −0.680 au). Compared with the product of the previous step, only a slight rotation of the substrate is observed. This rearrangement is almost thermoneutral (−1.8 kcal/mol) and barrierless (0.8 kcal/mol), and therefore we did not optimize its transition state because it was irrelevant for the global reaction. This rotation permits a closer contact between oxygen O6 of the substrate and the NH group of His306 (O6−H4 bond length 1.68 versus 2.62 Å in the previous step). The transition state of this reaction is characterized by an imaginary frequency of 213i cm^{-1} and reveals that the oxygen atom O6 is starting to dissociate from the tetrahedral intermediate (O6−C5 bond length of 1.79 versus 1.49 Å in the reactants) and very close to the NH group of His306 (O6−H4 bond length of 1.12 Å) at this stage. At the same time, the proton of Asp276 becomes closer to the Nδ atom of His306 (H2−N2 bond length of 1.62 versus 1.49 Å in the reactants). In the product of this reaction, the formation of the acyl−enzyme complex is completed, and the first product of the reaction, an alcohol molecule is released. In this structure, the oxygen atom of Ser169 shortens its distance within the acyl

dx.doi.org/10.1021/bi500934j | *Biochemistry* 2014, 53, 5820−5829

Table 1. Important Distances during the Formation of the Acyl−enzyme Complex When the Substrate Is an Ester (X = O), Amide (X = NH), and Thioester (X = S)

		distances X = O (Å)						
		O^1-H^2	H^2-N^2	N^3-H^4	H^4-O^4	H^4-X^6	O^4-C^5	C^5-X^6
step 1	R	1.60	1.06	1.60	1.02	2.89	2.33	1.33
	TS	1.53	1.09	1.16	1.36	2.44	1.88	1.37
	P	1.46	1.18	1.06	1.64	2.62	1.56	1.43
step 2	R	1.49	1.15	1.05	2.45	1.68	1.48	1.49
	TS	1.62	1.07	1.41	2.50	1.12	1.42	1.79
	P	1.68	1.06	1.76	3.15	1.00	1.33	3.00
		distances X = N (Å)						
		O^1-H^2	H^2-N^2	N^3-H^4	H^4-O^4	H^4-X^6	O^4-C^5	C^5-X^6
step 1	R	1.60	1.07	1.62	1.01	3.04	2.38	1.35
	TS	1.52	1.09	1.13	1.42	2.84	1.82	1.41
	P	1.46	1.11	1.05	1.65	2.59	1.53	1.48
step 2	R	1.52	1.09	1.09	2.50	1.65	1.48	1.52
	TS	1.57	1.08	1.23	2.49	1.37	1.46	1.54
	P	1.66	1.06	2.25	4.05	1.03	1.35	3.77
		distances X = S (Å)						
		O^1-H^2	H^2-N^2	N^3-H^4	H^4-O^4	H^4-X^6	O^4-C^5	C^5-X^6
step 1	R	1.65	1.06	1.79	1.00	3.85	3199.00	1.78
	TS	1.55	1.08	1.23	1.27	3.16	1.91	1.84
	P	1.45	1.12	1.05	1.67	2.97	1.52	1.93
step 2	R	1.54	1.09	1.09	3.34	1.99	1.35	3.73
	TS	1.61	1.07	1.34	3.90	1.64	1.34	4.04
	P	1.68	1.06	2.07	4.19	1.37	1.35	4.13

complex (O4−C5 bond length of 1.33), while the other oxygen atom of the substrate is hydrogen bonded to the three backbone nitrogen atoms of the residues that form the oxyanion hole (Gly92, Gly93, and Ala170). This step requires an activation energy of 13.2 kcal/mol, and a change of the overall energy of reaction of −10.4 kcal/mol.

As was mentioned previously, CEs catalyze the hydrolysis or transesterification of a broad spectrum of structurally diverse compounds including esters, thioesters, and amides producing a variety of alcohols, amines, and thiols. Till now, we have only described the mechanism when the substrate is an ester. However, changing the nature of the atom located at position 6 of the substrate (methyl propionate) to sulfur or nitrogen, we can easily evaluate the differences in the mechanism for a thioester (*S*-methyl propionate) or for an amide (*N*-methyl propionate) respectively.

The optimized geometries of the reactants of the two new reactions show that the binding pose of the thioester and the amide are very similar to the one adopted by the propyl acetate and observed in the X-ray structure of the plant CEs.[29] Additionally, the computational results show that there are no significant differences in the mechanism required for the formation of the acyl−enzyme complex. Whenever the substrate is an ester, thioester, or amide, the full process requires two steps and involves the formation of similar tetrahedral intermediates. The only differences in the mechanisms are in the products of the reaction that are released after the second step. If the substrate is an ester, it is released as an alcohol molecule (previously described), if the substrate is an amide, then the corresponding amine is released, and finally, if the substrate is a thioester, a thiol molecule is found. Table 1 shows the most important distances involved in the formation of the acyl−enzyme complex with the three substrates.

The computational results show that this process is more favorable when the ester is the substrate both from the thermodynamic (reaction energy) and from the kinetic (activation energy) point of view (Figure 3). When the substrate is a thioester or an amide, the reaction tends to become less favored. This occurs due to an increase in the activation energies on the order of ∼5 and ∼6 kcal/mol and because the reaction no longer is exergonic becoming instead endergonic: 10.8 kcal/mol if the substrate is a thioester and 6.0

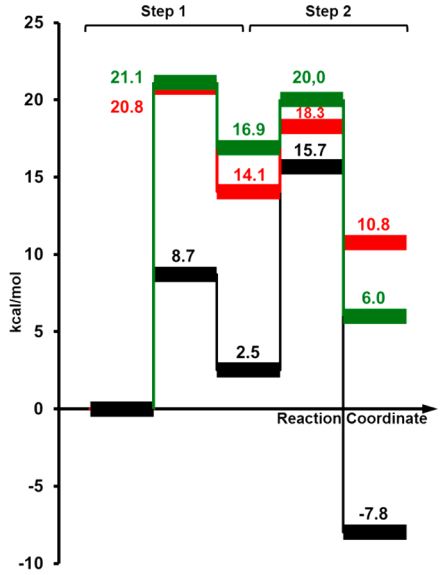

Figure 3. Energetics involved in the formation of the acyl−enzyme complex with the ester (black), thiolester (red), and amide (green) substrates.

dx.doi.org/10.1021/bi500934j | *Biochemistry* 2014, 53, 5820−5829

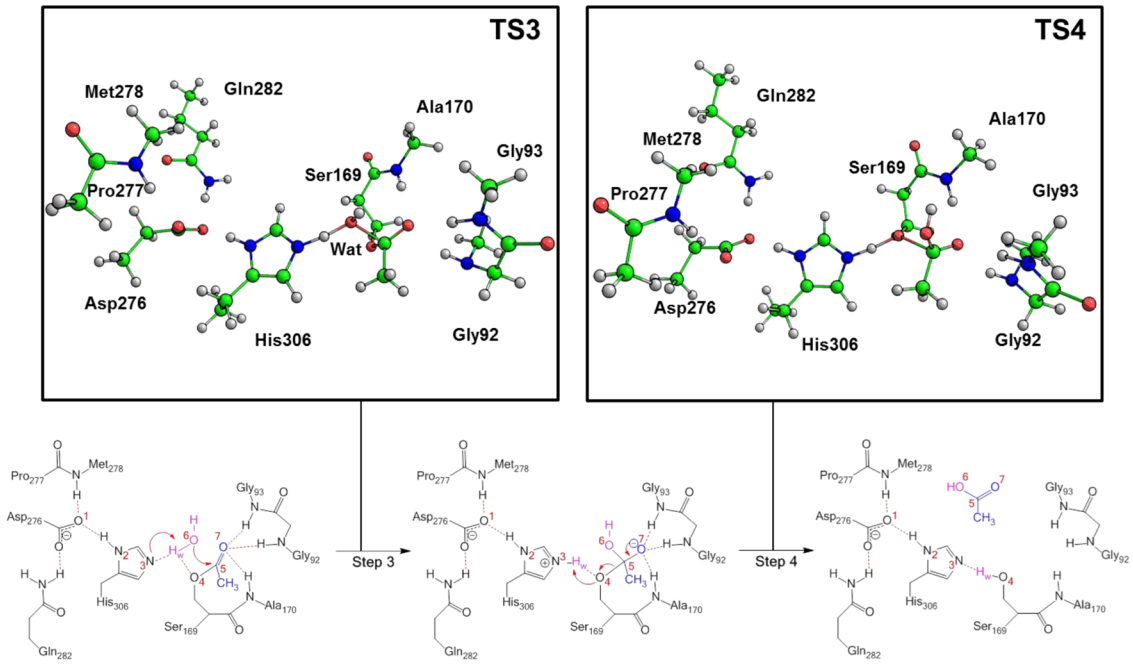

Figure 4. Schematic representation of the hydrolytic pathway and the corresponding TS structures.

kcal/mol if the substrate is an amide. These results reveal that bulkier atoms (sulfur atom or the NH group) attached to carbon C5 of the substrate hinder the formation of the tetrahedral intermediate, which scores a substantially higher energy. In addition, it is observed that the formation of the thiol and amine intermediates is less stable than the alcohol intermediate. This occurs due to the lower nucleophilic nature of the intermediates found from the thioester or the amide that hamper the release of the first product of the reaction.

Independently of the substrate that was studied, at the end of these two steps, Ser169 is covalently bonded to the acyl group of the initial substrate forming the acyl−enzyme complex. This means that, from this point, the hydrolytic mechanism or the transesterification reactions are equivalent for any of the three substrates, provided that the alcohol/thiol/amine product is released from the active site before the hydrolytic reaction takes place.

Hydrolytic Reaction. Once the formation of the acyl−enzyme complex is completed and a water molecule is available in the active site region, the hydrolytic reaction can take place. This reaction is essentially the reverse of the previous acylation step where the water molecule substitutes the organic group of the alcohol of the original substrate. Again, this reaction involves two sequential steps (Figure 4).

In the reactants of the first step, the water molecule occupies a similar position to that held by the alcohol molecule in the previous reaction. The position of the water molecule is stabilized by a hydrogen bond provided by the Nε atom of His306 (1.64 Å), and it is 2.44 Å away from carbon C5 of the substrate. Asp276 remains in the anionic form (total charge of −1.03 au) and in close contact with the NH group of His306 (O1−H2 bond length of 1.62 Å). The carbonyl group of the acyl complex continues to be stabilized by three hydrogen bonds provided by the glycine residues and alanine residue of the oxyanion pocket (with an averaged hydrogen bond distance of 1.99 Å). The transition state of this reaction is characterized by an imaginary frequency of 662i cm^{-1}. In this structure, the water molecule is already very close to carbon C5 of the acyl−enzyme complex (O6′−C5 bond length of 1.85 Å), and one hydrogen atom of the water molecule is already shared with one of the nitrogen atoms of His306 (H6−N3 bond length of 1.21 versus 1.64 Å in the reactants). Asp276 becomes closer to the other NH group of His306 (H2−O1 bond length 1.56 versus 1.62 Å in the reactants). In the products of this reaction, the hydroxyl group coming from the water molecule becomes attached to carbon C5 of the acyl−enzyme complex (O6′−C5 bond length of 1.53 Å). Asp276 is now closer to His306 (O1−H2 bond length 1.47 Å), and the charge is located mainly at the O7 of the substrate (partial charge of −0.992 au) and again stabilized by the nitrogen backbone atoms of glycine and alanine residues of the oxyanion pocket. The reaction requires an activation energy of 9.4 kcal/mol, and it is endergonic by 6.0 kcal/mol.

In the second step of the hydrolytic process, Ser169 disconnects from the acyl complex, and the active site is regenerated for a new catalytic cycle. In the reactants of this step, Ser169 is attached to carbon C5 of the substrate (O4−C5 bond length of 1.54 Å) and interacts very closely with the NH group of His306 (O4−H$_w$ bond length of 1.69 Å). In the transition state of this step (frequency 427i cm^{-1}), Ser169 is partially disconnected from the substrate (O4−C5 bond length of 1.91 Å), and the proton now belonging to His306 is halfway the path of the oxygen from Ser169 (H$_w$−O4 bond length 1.34 Å). The hydrogen bond formed between Asp276 and His306 is lengthened as histidine transfers the proton to the carboxylic acid (O1−H2 bond length of 1.54 versus 1.46 Å in the reactants). In the products of the reaction, the carboxylic acid is now free to dissociate from the active site, and Ser169 becomes protonated. Once the product dissociates from the active site, it becomes ready for new catalytic cycles. This reaction requires 3.8 kcal/mol, and it is exergonic in 14.0 kcal/mol. The potential energy profile for this reaction is shown in Figure 6.

Transesterification Reaction. When an alcohol is available in the active site, the transesterification pathway can take place instead of the hydrolytic process. This reaction is very similar to the hydrolytic process, but instead of exchanging the alcohol

dx.doi.org/10.1021/bi500934j | *Biochemistry* 2014, 53, 5820−5829

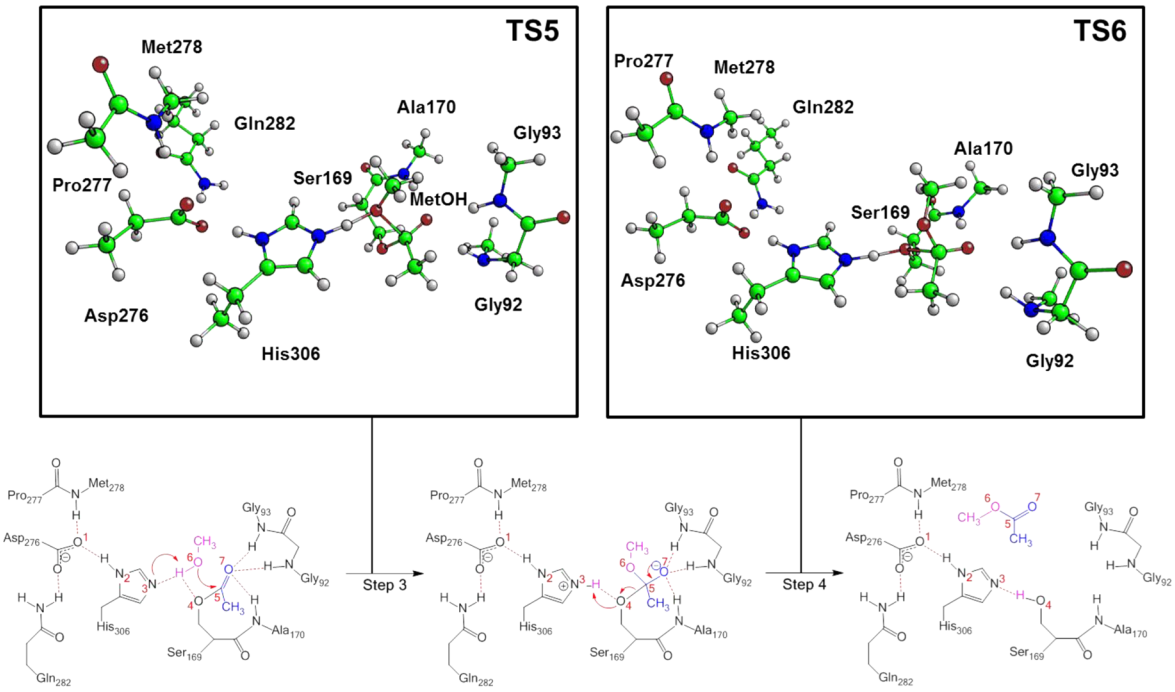

Figure 5. Schematic representation of the transesterification pathway and the corresponding TS structures.

group of the ester formed within the acyl−enzyme complex by a hydroxyl group (from the water molecule), it is exchanged by another alcohol group (Figure 5).

The optimized geometry of the reactants shows that the position of the alcohol molecule (in this case a methanol molecule) is stabilized between the acyl complex and His306. The hydroxyl group of the alcohol is pointing toward the Nε atom of His306 establishing a hydrogen bond (O6−H3 bond length of 1.74 Å). Such interaction allows the approach of the oxygen atom near carbon C5 of the acyl−enzyme complex (O6−C5 bond length of 2.81 Å) promoting in this way the transesterification process.

The transition state structure of the first step of this reaction is characterized by an imaginary frequency of 362i cm^{-1}. At this stage, the hydroxyl group of the alcohol is already very close to carbon C5 of the acyl−enzyme complex (O6−C5 bond length of 1.89 Å), and the hydrogen atom is shared with one of the nitrogen atoms of His306 (H6−N3 bond length of 1.16 versus 1.74 Å in the reactants). Asp276 is now closer to the Nδ atom of His306 (O1−H2 bond length of 1.56 versus 1.68 Å in the reactants). At the product of this step, the alcohol molecule becomes covalently bonded to the acyl−enzyme complex forming a tetrahedral intermediate that is negatively charged (total charge of −0.926 au). His306 accepts the proton from the hydroxyl group of the alcohol, decreasing the distance H6′−N3 from 1.16 to1.06 Å. This reaction requires an activation energy of 16.3 kcal/mol, and the reaction is endergonic by 12.0 kcal/mol.

The second step of the transesterification mechanism involves the release of the ester product and turnover of the active site. In the reactants, there is a small rotation of the acyl substrate that favors the proximity of the oxygen from Ser169 to the NH group of His306 (O4−H6′ bond length of 1.67 Å), while it is firmly attached to the tetrahedral acyl complex (O4−C5 bond length of 1.56 Å). The final complex remains negatively charged, and it is stabilized by two hydrogen bonds provided by the two glycines and the alanine of the oxanion hole. The transition state is characterized by an imaginary frequency at 361i cm^{-1}. In this state, Ser169 is partially dissociated from the substrate (1.89 versus 1.56 Å in the reactants). The proton that was previously attached to His306 is now shared with Ser169 (distance H6′−O4 of 1.358 Å and distance H6′−N3 of 1.16 Å). The hydrogen atom belonging to His306 and hydrogen bonded to Asp276 lengthens its distances H2−O1 from 1.46 Å in the reactant structure to 1.53 Å in the transition structure. In the product of the reaction, Ser169 is finally reprotonated and unbound from the substrate. The substrate is now free to dissociate from the active site, although the carbonyl group remains stabilized by hydrogen bond interactions with the oxyanion hole. The reaction requires an activation energy of 2.3 kcal/mol and is exergonic by 10.8 kcal/mol.

CONCLUSIONS

The computational results revealed that the reactions catalyzed by CEs are characterized by the following mechanism: the substrate binds to the active site, the first product is released (alcohol, thiol, or amide), the next substrate binds (a water or an alcohol), and another product is released (carboxylic acid or an ester). The computational results have shown however that the full process is achieved via a four-step reaction instead of two as it was previously described.[1,21,29]

The catalytic process is dependent on the catalytic triad formed by Ser169, His306, and Asp276. These residues interact through a sequence of hydrogen bonds that allow an easy proton transfer between Ser169 and His306, increasing the nucleophilic nature of Ser169, which otherwise is a poor nucleophile. The first step involves the transfer of a proton from the adjacent Ser169 to the opposing nitrogen of His306, from which results a nucleophilic oxygen that attacks the carbonyl carbon of the substrate. At the end of this step, Ser169 becomes covalently bonded to the substrate and forms the first of two tetrahedral intermediates of the catalytic process. In the second step of the mechanisms, the first products of these

dx.doi.org/10.1021/bi500934j | Biochemistry 2014, 53, 5820−5829

reactions are generated: if the reactant is an ester, the alcohol component of the ester is released, if it is a thioester, a thiol is released, and if the reactant is an amide, an amine is formed. This process occurs through the collapse of the tetrahedral intermediate, which is aided by the histidine, which acts as a general acid to produce an acyl−enzyme complex. The next steps of the mechanism are dependent on the availability of water or alcohol molecules in the active site. If a water molecule is available, then the hydrolytic reaction will take place, and the substrate will be converted into a carboxylic acid. If an alcohol is available instead, then the transesterification will take place, and at the end of the reaction, an ester product is obtained. In all of the cases, the mechanisms were found to be very similar. In the third step of the full mechanism, the acyl−enzyme complex is attacked by a histidine-activated water molecule (or alcohol molecule), which produces the second tetrahedral intermediate of the mechanism. This mechanism is the inverse of the previous step where the water molecule (or alcohol molecule) occupies the place of the released product and a proton is transferred from the latter to His306. The last step (fourth step of the full mechanism) involves the proton transfer from His306 to Ser169 followed by the concomitant release of the product of the reaction, a carboxylic acid or an ester depending on the conditions. Once this step is finished, the active site is regenerated and is ready for a new catalytic process.

The calculated Gibbs free energies for the studied reactions are displayed schematically in Figure 6. The formation of the

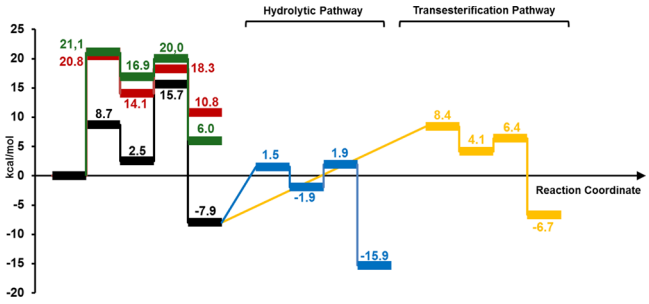

Figure 6. Full energetic pathway for the studied reactions catalyzed by CEs. Black, ester substrate; red, thioester substrate; green, amide substrate; blue, hydrolytic pathway; yellow, transesterification pathway.

acyl−enzyme intermediate is shown to be in all cases the rate-determining step. When the substrate is an ester, the second step, during which the bond to the leaving group is broken, is clearly the slowest one. The activation free energy found in this case agrees very well with the rate constant obtained experimentally (k_{cat} = 9.9 s^{-1}, ∼16.1 kcal/mol).[44] The results reveal that the full catalytic process is more favored when the substrate is an ester than when it is a thioester or an amide. The substitution of an oxygen atom of the ester substrate by a sulfur atom (in thioesters) increases the activation energy by 5 kcal/mol, and the full process becomes endergonic (10.8 kcal/mol) rather than exergonic as was observed with the normal substrate (−7.9 kcal/mol). This scenario is even less favorable when the substrate is an amide. Indeed, the exchange of an oxygen atom of the ester substrate by an NH group in amides leads to an increase of 6 kcal/mol in the activation energy, and the full process becomes endergonic (6.0 kcal/mol) in relation to the results that were obtained with the ester substrate. These results agree very well with the available experimental observations where the catalytic activity of CEs is more favorable with esters rather than when other types of substrates.[45,46]

Once the acyl−enzyme complex is obtained, there are two pathways from which the reactions can diverge: the hydrolytic and normal pathway or the transesterification pathway. Both mechanisms are similar whenever the substrate is an ester, a thiol, or an amide because after the formation of the acyl−enzyme complex and the release of the first product of the reaction (alcohol, thiol, or amide, respectively), the part of the substrate that remains bonded to the enzyme is common to all of them.

The calculated energies revealed that the hydrolytic pathway (normal pathway) is more favored from both the kinetic and thermodynamic point of view than the transesterification pathway. This is because the water molecule is a better nucleophile than the alcohol. However, the presence of alcohol molecules in higher concentrations than water can lead to the transesterification pathway. This means that when the substrate is an ester, both reactions should be competitive and the followed pathway may only be dependent on the presence of water or alcohol molecules in the active site. These results also agree with the available experimental data that have shown that although the transesterification reaction is not the normal pathway it can be efficiently catalyzed by CEs.[47−51] When the substrate is a thioester or an amide, this energetic profile is different. Higher barriers are found for the first two steps, but the subsequent hydrolytic or transesterification pathway depends on the delivery of the generated product in each case and the presence of water or alcohol molecules as mentioned before.

In summary, the computational results allow us to conclude that CEs can efficiently catalyze the hydrolysis and the transesterification of ester, thioester, and amide molecules, as well as explaining with atomistic detail why this is so. Both mechanisms can be competitive, and the only factor that dictates which one is followed is the abundance of water or alcohol molecules in the active site. The oxyanion cage formed by Gly92, Gly93, and Ala170 plays an important role in the reaction by stabilizing through two hydrogen bonds the negatively charged tetrahedral intermediates, in which the substrate becomes covalently bonded to Ser169.

Since CEs play an important role in the hydrolytic and transesterification of a vast number of structurally diverse drugs, we believe that the computational results obtained in this study will provide new insights about how these substrates are processed by these enzymes. This knowledge can now be used in the development of new drugs or for the improvement and understanding the pharmacokinetic behavior of existing therapeutic agents containing an ester, thioester, or amide bond.

■ ASSOCIATED CONTENT

Supporting Information

The coordinates of the starting cluster models for the study of the reaction of the propyl acetate, *S*-propyl ethanethioate, and *N*-propylacetamide. This material is available free of charge via the Internet at http://pubs.acs.org.

■ AUTHOR INFORMATION

Corresponding Authors

*E-mail: ignacio.tunon@uv.es.
*E-mail: mjramos@fc.up.pt.

Author Contributions

[§]J.A. and N.M.F.S.A.C. contributed equally to this work.

Notes

The authors declare no competing financial interest.

■ ACKNOWLEDGMENTS

J.A. thanks *La Caixa* for a master fellowship and *Ministerio de Economía y Competitividad* for a doctoral grant. N.M.F.S.A.C. thanks the program Ciencia2007. This work has been supported by FCT through the project EXCL/QEQ-COM/0394/2012.

■ REFERENCES

(1) Satoh, T., and Hosokawa, M. (1998) The mammalian carboxylesterases: From molecules to functions. *Annu. Rev. Pharmacol. Toxicol. 38*, 257−288.
(2) Potter, P. M., and Wadkins, R. M. (2006) Carboxylesterases - Detoxifying enzymes and targets for drug therapy. *Curr. Med. Chem. 13* (9), 1045−1054.
(3) Fleming, C. D., et al. (2005) Structural insights into drug processing by human carboxylesterase 1: Tamoxifen, mevastatin, and inhibition by benzil. *J. Mol. Biol. 352* (1), 165−177.
(4) Alexson, S. E. H., et al. (2002) Involvement of liver carboxylesterases in the in vitro metabolism of lidocaine. *Drug Metab. Dispos. 30* (6), 643−647.
(5) Quinney, S. K., et al. (2005) Hydrolysis of capecitabine to 5′-deoxy-5-fluorocytidine by human carboxylesterases and inhibition by loperamide. *J. Pharmacol. Exp. Ther. 313* (3), 1011−1016.
(6) Takai, S., et al. (1997) Hydrolytic profile for ester- or amide-linkage by carboxylesterases pI 5.3 and 4.5 from human liver. *Biol. Pharm. Bull. 20* (8), 869−873.
(7) Satoh, T., et al. (2002) Current progress on esterases: From molecular structure to function. *Drug Metab. Dispos. 30* (5), 488−493.
(8) Redinbo, M. R., and Potter, P. M. (2005) Mammalian carboxylesterases: From drug targets to protein therapeutics. *Drug Discovery Today 10* (5), 313−325.
(9) Tsujita, T., and Okuda, H. (1993) Palmitoyl-coenzyme A hydrolyzing activity in rat kidney and its relationship to carboxylesterase. *J. Lipid Res. 34* (10), 1773−1781.
(10) Becker, A., et al. (1994) Purification, Cloning, and Expression of a Human Enzyme with Acyl-Coenzyme-a - Cholesterol Acyltransferase Activity, Which Is Identical to Liver Carboxylesterase. *Arterioscler. Thromb. 14* (8), 1346−1355.
(11) Ghosh, S. (2000) Cholesteryl ester hydrolase in human monocyte/macrophage: cloning, sequencing, and expression of full-length cDNA. *Physiol. Genomics 2* (1), 1−8.
(12) Hosokawa, M., et al. (2007) Genomic structure and transcriptional regulation of the rat, mouse, and human carboxylesterase genes. *Drug Metab. Rev. 39* (1), 1−15.
(13) Diczfalusy, M. A., et al. (2001) Characterization of enzymes involved in formation of ethyl esters of long-chain fatty acids in humans. *J. Lipid Res. 42* (7), 1025−1032.
(14) Dolinsky, V. W., et al. (2001) The cloning and expression of a murine triacylglycerol hydrolase cDNA and the structure of its corresponding gene. *Biochim. Biophys. Acta, Mol. Cell Biol. Lipids 1532* (3), 162−172.
(15) Krishnasamy, S., et al. (1998) Molecular cloning, characterization, and differential expression pattern of mouse lung surfactant convertase. *Am. J. Physiol.: Lung Cell. Mol. Physiol. 275* (5), L969−L975.
(16) Miyazaki, M., et al. (2006) A major urinary protein of the domestic cat regulates the production of felinine, a putative pheromone precursor. *Chem. Biol. 13* (10), 1071−1079.
(17) Brzezinski, M. R., et al. (1997) Human liver carboxylesterase hCE-1: Binding specificity for cocaine, heroin, and their metabolites and analogs. *Drug Metab. Dispos. 25* (9), 1089−1096.
(18) Hosokawa, M., et al. (1995) Interindividual Variation in Carboxylesterase Levels in Human Liver-Microsomes. *Drug Metab. Dispos. 23* (10), 1022−1027.
(19) Redinbo, M. R., Bencharit, S., and Potter, P. M. (2003) Human carboxylesterase 1: from drug metabolism to drug discovery. *Biochem. Soc. Trans. 31*, 620−624.
(20) Sogorb, M. A., and Vilanova, E. (2002) Enzymes involved in the detoxification of organophosphorus, carbamate and pyrethroid insecticides through hydrolysis. *Toxicol. Lett. 128* (1−3), 215−228.
(21) Imai, T. (2006) Human carboxylesterase isozymes: Catalytic properties and rational drug design. *Drug Metab. Pharmacokinet. 21* (3), 173−185.
(22) Hosokawa, M. (2008) Structure and Catalytic Properties of Carboxylesterase Isozymes Involved in Metabolic Activation of Prodrugs. *Molecules 13* (2), 412−431.
(23) Frey, P. A., Whitt, S. A., and Tobin, J. B. (1994) A Low-Barrier Hydrogen-Bond in the Catalytic Triad of Serine Proteases. *Science 264* (5167), 1927−1930.
(24) Oliveira, E. F., et al. (2011) Mechanism of formation of the internal aldimine in pyridoxal 5′-phosphate-dependent enzymes. *J. Am. Chem. Soc. 133* (39), 15496−15505.
(25) Cerqueira, N.M.F.S.A., Fernandes, P. A., and Ramos, M. L. (2007) Understanding ribonucleotide reductase inactivation by gemcitabine. *Chem.—Eur. J. 13* (30), 8507−8515.
(26) Cerqueira, N.M.F.S.A., et al. (2009) The Effect of the Sixth Sulfur Ligand in the Catalytic Mechanism of Periplasmic Nitrate Reductase. *J. Comput. Chem. 30* (15), 2466−2484.
(27) Mota, C. S., et al. (2011) The mechanism of formate oxidation by metal-dependent formate dehydrogenases. *J. Biol. Inorg. Chem. 16* (8), 1255−1268.
(28) Ramos, M. J., and Fernandes, P. A. (2008) Computational enzymatic catalysis. *Acc. Chem. Res. 41* (6), 689−698.
(29) Ileperuma, N. R., et al. (2007) High-resolution crystal structure of plant carboxylesterase AeCXE1, from *Actinidia eriantha*, and its complex with a high-affinity inhibitor paraoxon. *Biochemistry 46* (7), 1851−1859.
(30) Himo, F. (2006) Quantum chemical modeling of enzyme active sites and reaction mechanisms. *Theor. Chem. Acc. 116* (1−3), 232−240.
(31) Siegbahn, P. E. M., and Himo, F. (2011) The quantum chemical cluster approach for modeling enzyme reactions. *Wiley Interdiscip. Rev.: Comput. Mol. Sci. 1* (3), 323−336.
(32) Toscano, M. D., Woycechowsky, K. J., and Hilvert, D. (2007) Minimalist Active-Site Redesign: Teaching Old Enzymes New Tricks. *Angew. Chem., Int. Ed. 46* (18), 3212−3236.
(33) Frisch, M. J.; Trucks, G. W.; Schlegel, H. B.; Scuseria, G. E.; Robb, M. A.; Cheeseman, J. R.; Scalmani, G.; Barone, V.; Mennucci, B.; Petersson, G. A.; Nakatsuji, H.; Caricato, M.; Li, X.; Hratchian, H. P.; Izmaylov, A. F.; Bloino, J.; Zheng, G.; Sonnenberg, J. L.; Hada, M.; Ehara, M.; Toyota, K.; Fukuda, R.; Hasegawa, J.; Ishida, M.; Nakajima, T.; Honda, Y.; Kitao, O.; Nakai, H.; Vreven, T.; Montgomery, J. A., Jr.; Peralta, J. E.; Ogliaro, F.; Bearpark, M.; Heyd, J. J.; Brothers, E.; Kudin, K. N.; Staroverov, V. N.; Kobayashi, R.; Normand, J.; Raghavachari, K.; Rendell, A.; Burant, J. C.; Iyengar, S. S.; Tomasi, J.; Cossi, M.; Rega, N.; Millam, J. M.; Klene, M.; Knox, J. E.; Cross, J. B.; Bakken, V.; Adamo, C.; Jaramillo, J.; Gomperts, R.; Stratmann, R. E.; Yazyev, O.; Austin, A. J.; Cammi, R.; Pomelli, C.; Ochterski, J. W.; Martin, R. L.; Morokuma, K.; Zakrzewski, V. G.; Voth, G. A.; Salvador, P.; Dannenberg, J. J.; Dapprich, S.; Daniels, A. D.; Farkas, O.; Foresman, J. B.; Ortiz, J. V.; Cioslowski, J.; Fox, D. J. *Gaussian 09, Revision C.01*; Gaussian, Inc.: Wallingford, CT, 2009.
(34) Hohenberg, P., and Kohn, W. (1964) Inhomogeneous Electron Gas. *Phys. Rev. B 136* (3B), B864.
(35) Becke, A. D. (1993) A New Mixing of Hartree-Fock and Local Density-Functional Theories. *J. Chem. Phys. 98* (2), 1372−1377.
(36) Lee, C. T., Yang, W. T., and Parr, R. G. (1988) Development of the Colle-Salvetti Correlation-Energy Formula into a Functional of the Electron-Density. *Phys. Rev. B 37* (2), 785−789.

(37) Stephens, P. J., et al. (1994) Ab-Initio Calculation of Vibrational Absorption and Circular-Dichroism Spectra Using Density-Functional Force-Fields. *J. Phys. Chem. 98* (45), 11623−11627.
(38) Rassolov, V. A., et al. (2001) 6-31G*basis set for third-row atoms. *J. Comput. Chem. 22* (9), 976−984.
(39) Zhao, Y., and Truhlar, D. G. (2008) Density functionals with broad applicability in chemistry. *Acc. Chem. Res. 41* (2), 157−167.
(40) Zhao, Y., and Truhlar, D. G. (2008) The M06 suite of density functionals for main group thermochemistry, thermochemical kinetics, noncovalent interactions, excited states, and transition elements: two new functionals and systematic testing of four M06-class functionals and 12 other functionals. *Theor. Chem. Acc. 120* (1−3), 215−241.
(41) Scalmani, G., and Frisch, M. J. (2010) Continuous surface charge polarizable continuum models of solvation. I. General formalism. *J. Chem. Phys. 132* (11), No. 114110.
(42) Cerqueira, N.M.F.S.A., et al. (2004) Ribonucleotide activation by enzyme ribonucleotide reductase: Understanding the role of the enzyme. *J. Comput. Chem. 25* (16), 2031−2037.
(43) Cerqueira, N.M.F.S.A., et al. (2006) Dehydration of ribonucleotides catalyzed by ribonucleotide reductase: The role of the enzyme. *Biophys. J. 90* (6), 2109−2119.
(44) Stok, J. E., et al. (2004) Investigation of the role of a second conserved serine in carboxylesterases via site-directed mutagenesis. *Arch. Biochem. Biophys. 430* (2), 247−255.
(45) Mentlein, R., and Heymann, E. (1984) Hydrolysis of ester- and amide-type drugs by the purified isoenzymes of nonspecific carboxylesterase from rat liver. *Biochem. Pharmacol. 33* (8), 1243−1248.
(46) Huang, T. L., et al. (1996) Structure-activity relationships for substrates and inhibitors of mammalian liver microsomal carboxylesterases. *Pharm. Res. 13* (10), 1495−1500.
(47) Kamendulis, L. M., et al. (1996) Metabolism of cocaine and heroin is catalyzed by the same human liver carboxylesterases. *J. Pharmacol. Exp. Ther. 279* (2), 713−717.
(48) Laizure, S. C., et al. (2003) Cocaethylene metabolism and interaction with cocaine and ethanol: Role of carboxylesterases. *Drug Metab. Dispos. 31* (1), 16−20.
(49) Markowitz, J. S., et al. (2000) Ethylphenidate formation in human subjects after the administration of a single dose of methylphenidate and ethanol. *Drug Metab. Dispos. 28* (6), 620−624.
(50) Sai, K., et al. (2001) A new metabolite of irinotecan in which formation is mediated by human hepatic cytochrome P-450 3A4. *Drug Metab. Dispos. 29* (11), 1505−1513.
(51) Tang, B. K., and Kalow, W. (1995) Variable Activation of Lovastatin by Hydrolytic Enzymes in Human Plasma and Liver. *Eur. J. Clin. Pharmacol. 47* (5), 449−451.